Turkish Journal of Electrical Engineering & Computer Sciences

http://journals.tubitak.gov.tr/elektrik/

Research Article

Turk J Elec Eng & Comp Sci
(2018) 26: 2374 – 2384

doi:10.3906/elk-1710-133

Diode clamped gate driver-based high voltage pulse generator for electroporation

Krishnaveni SUBRAMANI*, **Rajini VEERARAGHAVALU**
Department of Electrical and Electronics, Faculty of Engineering, Sri Siva Subramanya Nadar College of Engineering, Chennai, Tamil Nadu, India

Received: 13.10.2017 • **Accepted/Published Online:** 18.06.2018 • **Final Version:** 28.09.2018

Abstract: Pulsed electric field technology is an emerging nonthermal food processing method. PEF food processing requires a high voltage pulse generator that produces high intensive pulses to be delivered to the food product. Innovation in semiconductor technology motivates researchers to modernize high voltage pulse generators to reduce the cost, size, and complexities in circuit operation and to increase the suitability for food processing since the last few decades. The present study aims to explore a high voltage pulse generator for electroporation study. The implemented high voltage pulse generator develops ∼1.62 kV with adjustable pulse widths of 0.62 μs and 1.2 μs. The pulse frequency can be adjusted to 1, 10, 20, and 51 kHz by using a preprogrammed microcontroller. The implemented pulse generator is simple and compact at affordable cost. Experiments were conducted to prove the feasibility of the implemented high voltage pulse generator to inactivate *Escherichia coli* microorganisms. *Escherichia coli* cells were exposed to the electric field intensity produced by the implemented pulse generator and the observed results showed that there is a significant reduction of 5.9 log scale from the initial concentration.

Key words: Pulsed electric field, pulse repetitive frequency, power MOSFETs, electroporation, resonant inductor

1. Introduction

Nowadays, every individual is aware of the taste, color, flavor, and nutritional value of the food that he/she consumes. However, it may not always be possible to taste fresh food throughout the year due to the seasonal changes and this leads researchers to innovate with new food processing techniques. Generally, thermal food processing methods are used in the food industry to increase shelf life and maintain food safety by inactivating pathogenic and spoilage microorganisms. Though thermal methods satisfy the food needs, the heat involved in the methods (normally above 60 °C) may degrade the nutrients, flavor, and color. This point motivated researchers to explore a new area in the field of food processing technology, which has turned the world's attention towards nonthermal food processing methods.

The pulsed electric field (PEF) method is one of the most attractive methods among all other nonthermal methods and this method provides safe, nutritious, and fresh-like quality food [1-5]. A large number of investigations in the food industry showed that the PEF process has the ability to inactivate microbes at low temperatures and hence minimizes deleterious heat effects on food [6,7].

*Correspondence: krishnavenis@ssn.edu.in

2. Electroporation in food processing method

A basic understanding of food pasteurization mechanisms is very helpful in improving PEF generator design, and the electroporation mechanism is reviewed briefly as follows. Electroporation is the process of structural changes in the membrane surface of microorganisms when they are subjected to high intensity pulses [8]. Electroporation inactivates the microorganisms suspended in liquid food when the cell outer membrane voltage is greater than the threshold membrane voltage, typically 1 V. In order to design any PEF generator, electrical parameters like electric field intensity, pulse width, pulse shape, and repetition rate are important and must be properly determined to inactivate the microorganisms effectively. In addition to this, the degree of bacterial decontamination is related to the product of pulse width and pulse frequency [9-11]. When the frequency is increased to 10 to 1 MHz, the voltage across the outer cell membrane decreases and approaches a very small value at microwave frequency [12-14]. It can be stated that the outer membrane capacitance works as a short circuit at higher frequencies and the applied voltage directly acts on the inner part of the cell. Hence, proper selection of pulse frequency enhances the inactivation level at moderate electric field intensity itself.

2.1. Developments in PEF generators

The PEF generator is one of the main subsystems of the PEF food processing method. High intensity pulses could be generated by several well-known classical techniques [15]. The PEF generator generally consists of one or more power supplies, switches, passive components, and a treatment chamber [16-18]. PEF generators can be classified either based on the circuit operation or the switches that play a key role. PEF generators can be broadly classified into two categories with respect to the switch abilities as ON switches and ON/OFF switches. The thyratrons, ignitrons, gas spark gaps, and trigatrons are a few examples of ON switches and these switches can handle high voltage at an affordable cost. However, classical ON type switches have drawbacks as follows: i) the repetition rate is limited, usually less than 100 Hz; ii) the complexity is greater in designing the triggering circuits; iii) time delays are introduced during ON/OFF operation, which in turn increases the rise time and fall time and may alter the wave shape; iv) switches are limited regarding the maximum energy delivered per pulse. However, technological upgrades in semiconductor devices have been introduced in PEF systems to make them efficient. The IGBT, thyristor, and MOSFET are a few familiar ON/OFF switches and improvements in solid state devices have also resulted in longer life with better performance. These advanced semiconductor devices require less complex driving circuits. They are easy to handle and control by external triggering and optimum variability of pulse parameters. Pulse repetition frequency of the standard switches can reach up to several kHz and makes the solid state switches very suitable for industrial scale applications. However, modernized PEF generators, which consist of specially designed power devices like a laser-activated thyristor, semiconductor closing switches, semiconductor opening switches, and fast recovery drift diodes, need auxiliary circuits to work in the operating region without sacrificing their good precision [19-21].

Unlike the PEF generators reported in [19-21], PEF generators can be designed by using semiconductor devices available on the market, which do not require any additional design features. Well-familiarized mass manufactured MOSFET devices with voltage/current ratings limited to $\sim$100 V and $\sim$10 A can be used for higher voltage/current ratings by connecting the MOSFETs either in series or parallel. However, they need a proper MOSFET driver circuit to turn on the MOSFETs simultaneously.

Generally, the applied electric field intensity needs to be in the range of 10–40 kV/cm to inactivate microorganisms by delivering the requiring electrical energy. The electrical energy can be increased either by

increasing the PEF generator voltage or by increasing the pulse repetition frequency. As the cost of the PEF generator is determined by its output voltage, the pulse repetition frequency can be increased to deliver the required electrical energy instead of increasing the voltage. The prototype generator implemented by Flisar et al. [22] was able to deliver an average power of 250 W for 1 Hz and 2500 W for 10 Hz at 5 kV with 1 ms square wave pulses. However, the average power can be increased by increasing the pulse frequency even at lesser voltage. Shorter pulses in the submicrosecond range deliver electrical energy in mJ/pulse and reduce the thermal effects at a considerable rate [23].

The aim of this work was to develop a laboratory scale high voltage pulse generator by utilizing commercially available MOSFETs. It is also aimed to generate high frequency pulses to increase the average power at lower voltages and to design a suitable driver circuit. Section 1.1 described the mechanism of microbial inactivation in liquid food by the PEF method, and the developments of the PEF generator have been briefly explained in Section 1.2. Section 2 describes the implementation of the PEF generator. The PEF electrical characteristics and performance of inactivating the bacteria are discussed in Section 3. Finally, Section 4 concludes the work with the future scope of PEF generator design.

3. Materials and methods

3.1. Design of the proposed high voltage pulse generator

Narrower high-intensity pulses are generated using the proposed MOSFET pulse generator, which is shown in Figure 1. The high voltage pulse generator consists of two parts: a diode clamped gate driver circuit (DCGD) and the high voltage pulse generator.

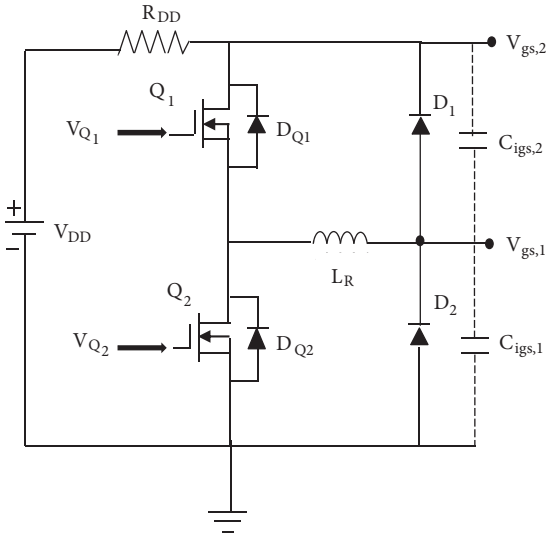

Figure 1. DCGD circuit.

3.2. Design of diode clamped gate driver

High switching frequency MOSFETs are required to meet the demand of high power density, compactness, and high repetitive pulse frequency. High switching frequency allows minimizing the volume of the passive components used in the circuit, such as inductors, transformers, and capacitors, but high frequency operation

leads to higher losses in the systems, and about 30% to 40% of the total losses occur in the gate driver circuits themselves [24]. The efficiency can be improved by a proper design of the gate driver circuit to reduce the switching losses in the case of high frequency applications. This can be done by introducing the energy recovery concept in the gate driver circuit design, which may help to increase the overall efficiency by supplying some portion of the energy returned back to the supply [25,26].

A driver circuit that is suitable for high frequency operation to trigger two MOSFETs was described by the authors in [27]. The driver circuit mentioned in [27] is used to generate high voltage pulses with adjustable frequency and the results of electroporation are presented here.

The DCGD circuit is shown in Figure 1, where the junction node of the driving pair of MOSFETs, Q_1 and Q_2, is connected to the resonant inductor (L_R). The body diodes of Q_1 and Q_2 are represented as D_{Q1} and D_{Q2}, as shown in Figure 1, and two more diodes, D_1 and D_2, are included additionally to clamp the voltage. Diodes D_1 and D_2 are used to recover the electrical energy by providing a low impedance path for the gate driver current. The input gate-source capacitances of power MOSFETs M_1 and M_2 are represented by $C_{igs,1}$ and $C_{igs,2}$, respectively. The internal gate resistance of MOSFETs M_1 and M_2 can be represented as D_G, which acts as the damping resistance in the second order circuit, not shown in Figure 1.

MOSFETs Q_1 and Q_2 are triggered at uniform intervals by applying control pulses and the control pulses are generated using a preprogrammed microcontroller. The control pulses on Q_1 and Q_2 are applied in such a way that Q_1 and Q_2 should not be turned on simultaneously. Thus, the cross-conduction loss is reduced significantly by avoiding the shoot-through between Q_1 and Q_2.

The DCGD circuit operation can be explained with the help of the waveforms shown in Figures 2a–2d, which can be divided into several phases corresponding to time periods from t_0 to t_8.

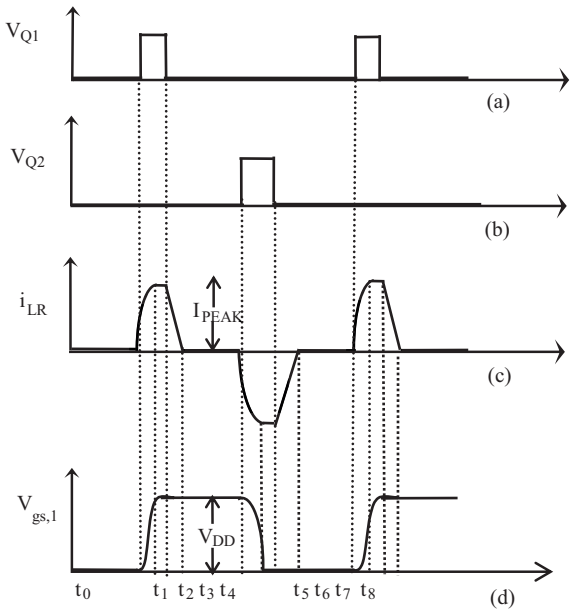

Figure 2. DCGD circuit key waveforms: a- control pulse of MOSFET Q_1, b- MOSFET Q_2, c- current through resonance inductor i_{LR}, d- gate-source voltage of power MOSFET M_1.

Phase I: It is assumed that initially no pulses are applied to MOSFETs Q_1 and Q_2. At the time of t_1, the control pulse is asserted on Q_1 and immediately Q_1 is turned on. As soon as Q_1 is turned on, the inductor

current (i_{LR}) flows through inductor L_R and it develops the voltage across $C_{igs,1}$ ($V_{gs,1}$) until the time period of t_2. As long as Q_1 is turned on, the resonance is built up along L_R and $C_{igs,1}$. $V_{gs,1}$ will rise towards the DCGD supply voltage (V_{DD}) and i_{LR} will rise towards the peak current (I_{PEAK}). Whenever $V_{gs,1}$ exceeds V_{DD}, diode D_1 conducts and prevents further charging of $C_{igs,1}$. After the time period of t_2, current i_{LR} starts to flow through the conduction path of $D_1 - Q_1 - L_R - D_1$ and continues until the time period of t_3. The instantaneous current (i_{LR}) and voltage ($V_{gs,1}$) can be derived by solving the second order circuit and can be expressed as in Eqs. (1) and (2).

$$i_{LR}(t) = \frac{2V_{DD}}{\sqrt{\frac{4L_R}{C_{igs,1}} - R_G^2}} e^{\frac{-R_G}{L_R}t} \sin\left(\frac{\sqrt{\frac{4L_R}{C_{igs,1}} - R_G^2}}{2L_R}\right) \tag{1}$$

$$V_{gs,1}(t) = \int_0^t \frac{1}{C_{igs,1}} i_{LR}(t)\, dt \tag{2}$$

The I_{PEAK} and rise time (t_r) can be readily estimated if the quality factor of the resonant circuit is good enough and gate resistance R_G of MOSFET M_1 is very small.

$$I_{PEAK} = V_{DD} \times \sqrt{\frac{C_{igs,1}}{L_R}} \tag{3}$$

$$t_r = \frac{\pi}{2}\sqrt{C_{igs,1}L_R} \tag{4}$$

Phase II: At time t_3, Q_1 is turned off but still current i_{LR} continues to flow due to the energy stored in inductor L_R. Thus, i_{LR} takes the current path of $D_1 - V_{DD} - D_{Q2} - L_R - D_1$ and dies out slowly. The stored magnetic energy in L_R is transferred to the DCGD supply during this time period of t_3 to t_4. Although the energy recovered per single control pulse is very small, it would reduce a significant amount of power in the case of high frequency applications.

Phase III: During the time period of t_4 to t_5, there are no current flows through inductor L_R, and $V_{gs,1}$ holds its maximum voltage. As soon as Q_2 is turned on at time t_5, again the resonance builds up through Q_2, L_R, and $C_{igs,1}$. $C_{igs,1}$ starts to discharge the voltage from its maximum value and so now i_{LR} flows through the path $C_{igs,1} - L_R - Q_2 - C_{igs,1}$, which is the opposite direction of i_{LR} during the Phase I period. The other clamping diode, D_2, prevents $V_{gs,1}$ from decreasing below zero due to the resonance and forces i_{LR} to flow through $D_2 - L_R - Q_2 - D_2$ during the time period of t_6 to t_7.

Phase IV: If MOSFET Q_2 is turned off at time t_7, i_{LR}, which still flows, takes the conduction path of $C_{igs,1} - L_R - D_{Q1} - V_{DD} - C_{igs}$ and dies out slowly. Again, during the time period of t_7 to t_8, the magnetic energy stored in L_R is returned to the DCGD supply. Thus, the capacitor charging and discharging behavior develops the required gate-source voltage pulses ($V_{gs,1}$ and $V_{gs,2}$).

3.3. High voltage pulse generation

Power MOSFETs M_1 and M_2 are connected in series with the source inductor, L_S, and energized by the DC supply (V_S) as shown in Figure 3. Whenever $V_{gs,1}$ is maximum, it turns on MOSFET M_1, and it also initiates

M_2 to be turned on. Thus, M_1 and M_2 are switched ON simultaneously. When $V_{gs,1}$ drops down to zero voltage, it turns off M_1 and makes the source terminal of M_2 (S_{M2}) be virtually floating. The interruption of the source inductor current (i_{LS}) by turning on and off switches M_1 and M_2 generates high voltage pulses. The number of MOSFETs connected in series can be determined based on the voltage rating of the selected MOSFET and the maximum voltage developed by the high voltage pulse generator. The current through the inductor, L_S, is expressed by Eq. (5).

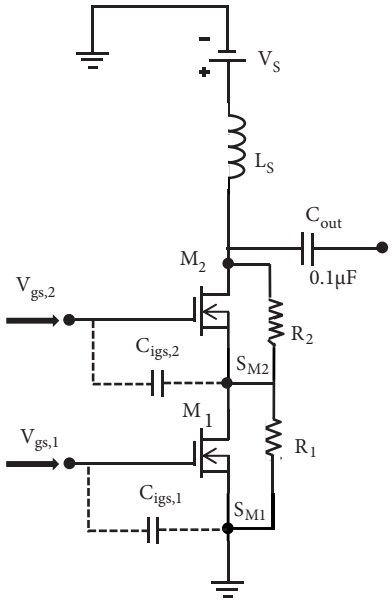

Figure 3. High voltage pulse generator.

$$i_{LS}(t) = \frac{1}{L_S}\int v_{LS}(t)\, d(t) \tag{5}$$

If the drain-source resistance (R_{DS}) of M_1 and M_2 is very small, the voltage drop across the switches can be neglected. The maximum source current is obtained by using Eq. (2) with zero initial currents, as shown in Eq. (6).

$$I_{LS,\,\max} = \frac{V_L}{L}\Delta t_{on} \tag{6}$$

If MOSFETs M_1 and M_2 are turned on for a short period, i_{LS} is not allowed to reach the steady state value. i_{LS} initially flows in the forward direction when M_1 and M_2 are turned on and it reverses its direction when M_1 and M_2 are turned off suddenly for a short time period. Due to the sudden interruption of the source current, voltages of several kV/device are generated. The generated pulse voltage and pulse length are determined by the inductor value and di/dt rating of the MOSFET. When the source inductor value and input voltage are varied, the corresponding output voltage is also varied. It shows that the current rises/falls rapidly and increases the output voltage drastically for the smaller inductance value. The pulse length can be shortened and peak voltage can be increased by choosing a proper source inductor.

4. Experimental setup

The experimental setup is shown in Figure 4.

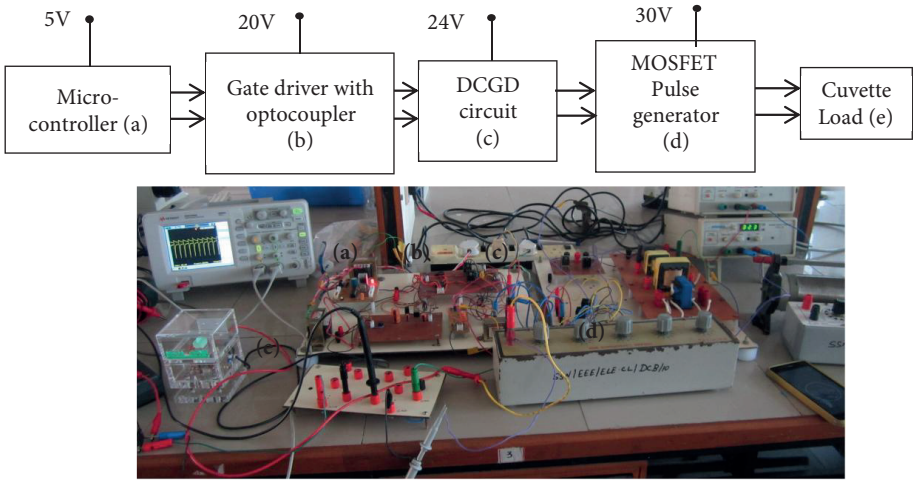

Figure 4. Experimental setup.

4.1. Circuit description

The two control pulses of magnitude 5 V with precise pulse duration were generated using a microcontroller and delays were introduced between the two control pulses. The PIC18F2550 was programmed to generate 20 μs pulses with a pulse length of 4 μs. The PIC18F2550 was energized by a 5 V DC supply and the supply was built by using a bridge rectifier (Diode 1N4007) along with a voltage regulator (IC 7805).

The control pulses generated by the PIC18F2550 were used to trigger Q_1 and Q_2. These HEXFET IRF150N MOSFETs are suitable for higher switching speed with dynamic dv/dt rating. These MOSFETs were isolated from the microcontroller by using a gate driver with optocoupler IC (HCPL3120), which uses a 12 V power supply. This adapted DCGD driver simplifies the board layout. The high voltage pulse generator consists of two power MOSFETs, 2SK727-9520, each rated at 900 V, connected in series (M_1 and M_2). The DCGD was able to supply the current to charge the internal capacitance of M_1 and M_2 and the capacitance value ranged from 1500 to 2400 pF. The pulse generator was designed for an input power range of 60–240 W at the input voltage range of 30–120 V, 2 A, using the driver circuit reported in [27].

4.2. Experimental results

The outputs were measured using an Agilent Digital Storage Oscilloscope, X 3024A, with 200 MHz of 2 GSa/s. A small resistor of 100 Ω was inserted in series with L_R along with a small capacitor of 2.2 μF to make source terminal voltage Q_1 be stable during the pulse generation. The DCGD produces sufficient current to trigger the power MOSFETs.

The two power rheostats of 100 Ω were connected in parallel and used as a load for the generator to study the electrical characteristics of the implemented generator. The output voltages were measured for different source inductors using a high voltage 1000:1 passive probe and the details are shown in Figure 5.

The high voltage pulse generator developed by Grenier [28] used series connected MOSFETs, but required high input voltage to produce the high voltage pulses. The proposed PEF generator produces high output voltage

in the range of 400 V to 1.6 kV when the input voltage is in the range of 30–120 V DC. This is achieved by using the source inductor placed in series with the input source. The electrical energy delivered to the food product can also be increased by increasing the pulse frequency and the pulse length; the results are shown in Figure 6.

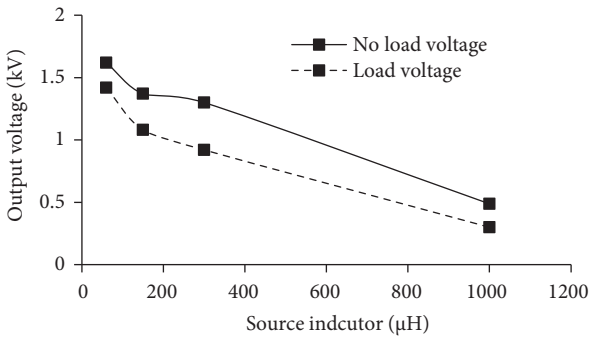

Figure 5. Output voltage of the PEF generator for different source inductors.

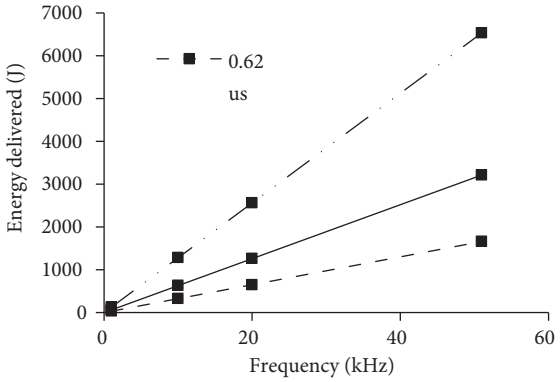

Figure 6. Energy delivered to the food product.

Though the power MOSFETs are triggered by 3.92 μs pulses, the source inductor majorly influences the pulse length of the output voltage. The pulse length varies in the range of 0.62–7 μs when the source inductor value is adjusted from 60 to 1000 μH.

The pulse generator output is shown in Figure 7, where the consecutive voltage pulses along with the corresponding single pulse are shown. The generated pulse has a flat top of width $\sim$1.2 μs with fast rise time. The pulse repetition frequency was 51 kHz.

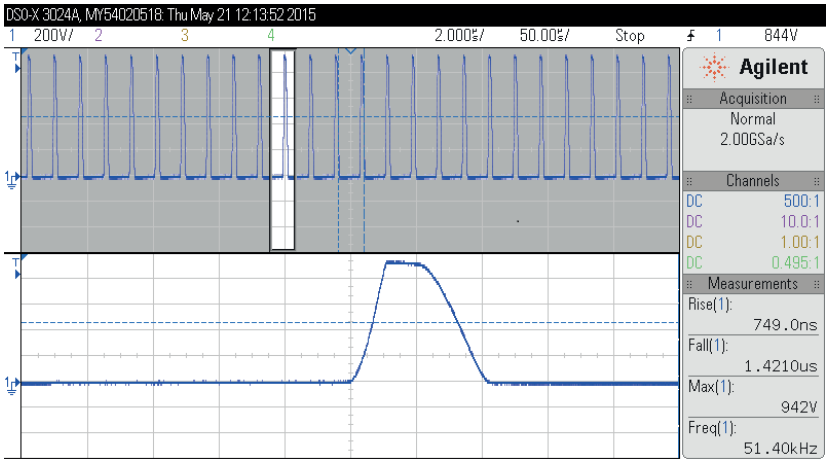

Figure 7. Output voltage of high voltage pulse generator.

The output voltage was distributed among the two MOSFETs, M_1 and M_2, which are connected in series. It was observed that when the input voltage was raised slowly the voltage was initially developed across the lower MOSFET, M_1, and when the voltage across M_1 crossed the rated voltage, the output voltage was shared by upper MOSFET M_2. The pulse frequency can be varied to 1, 10, 20, and 51 KHz with the preprogrammed PIC18F2550.

The suitability of the implemented pulse generator was verified by conducting experiments on inactive *Escherichia coli* bacteria inoculated in buffer solution. *E. coli* MTCC 1610 was collected from the Institute of Microbial Technology (Chandigarh) Microbial Type Culture Collection and GenBank. The strain was prepared as per the protocol and kept at –4 °C. The strain was brought to room temperature before the PEF treatment. An amount of 200 μL of sample strain was taken in a small electroporation cuvette and subjected to voltage of 1.62 kV for 1.2 μs at 51 kHz. The distance between the electrodes in the cuvette was set at 1 mm so that the PEF generator could develop electric field intensity of 16.2 kV/cm. The experiment was repeated in triplicate for different periods of 5 s, 10 s, 15 s, 20 s, and 30 s. The results are presented by considering the mean values. The temperature was measured before and after the treatment and the treatment temperature was ensured to be below 60 °C. The treated sample was streaked on nutrient agar plates and incubated overnight at 37 °C. Colony forming units (CFUs) were counted by using a digital colony counter. Images of nutrient agar plates are shown in Figure 8 when the *E. coli* microorganisms were treated by applying PEF for a time period of 30 s at 1 kHz, 10 kHz, and 51 kHz. It can be noticed clearly that CFUs were reduced at the higher frequency of 51 kHz, so the experimental results at 51 kHz are presented in Figure 9. It has been observed that cell viability counts were reduced from 7 log scales to 1.1 log scales with increased processing time in the present work, as shown in Figure 9.

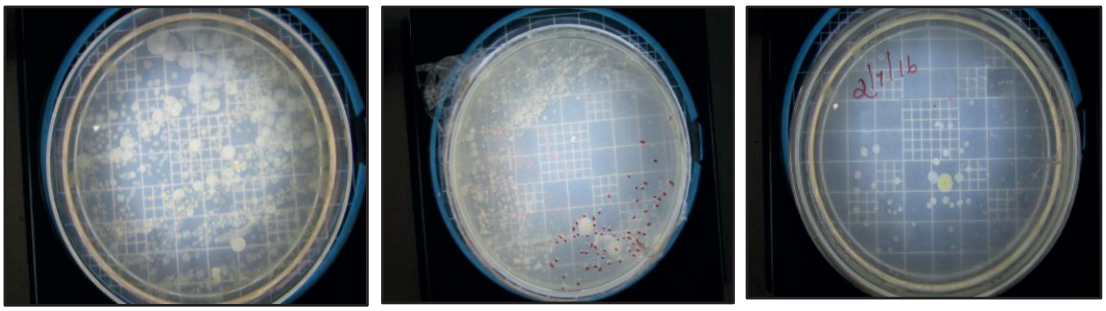

Figure 8. *E. coli* CFUs on agar plates treated by PEF after 30 s at frequencies of a) 1 kHz, b) 10 kHz, and c) 51 kHz.

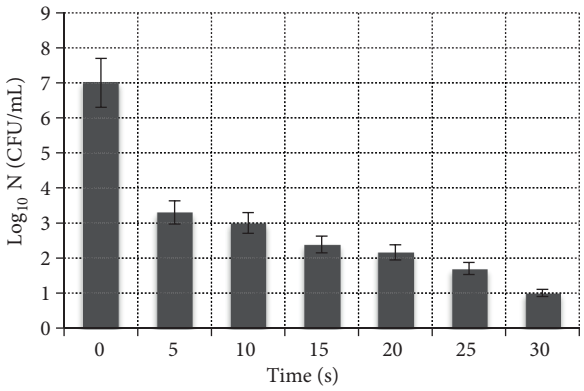

Figure 9. Survival reduction of *E. coli*.

This shows that the proposed laboratory scale high voltage pulse generator is suitable for the inactivation of bacteria and can be used in further electroporation studies. The implemented generator is a compact, portable, and cost-effective generator developed in the laboratory.

5. Conclusion

A high voltage pulsed power generator was designed, implemented, and used to inactivate *E. coli*. The high voltage generator produced 1.62 kV at different pulse frequencies. The control pulse width and frequency by the DCGD are flexible parameters and can be modified by a preprogrammed PIC18F2550. The number of MOSFETs associated with the high voltage pulse generator can be increased to improve the voltage magnitude or to reduce the voltage stress on each individual MOSFET, but care must be taken to use a well-synchronized method of triggering the individual MOSFETs. The other way to elevate the output voltage can be increasing the DC input voltage along with the appropriate design of the source inductor. The proposed PEF generator is compatible with commercial electroporation cuvettes. Hence, modularization of the implemented high voltage pulse generator helps in commercial production and the pulse parameters can also be easily modified to suit the requirements. Comparing the prototype implemented by Flisar et al. [22], the proposed one is capable of delivering higher average power by increasing the pulse frequency.

References

[1] Mohamed MEA, Eissa AHA. Pulsed electric fields for food processing technology. In: Eissa AHA, editor. Structure and Function of Food Engineering. Rijeka, Croatia: InTech Open Press, 2012. pp. 275-306.

[2] Min S, Evrendilek GA, Zhang HQ. Pulsed electric fields: processing system, microbial and enzyme inhibition and shelf life extension of foods. IEEE T Plasma Sci 2007; 35: 59-73.

[3] Buckow R, Sieh NG, Toepfl S. Pulsed electric field processing of orange juice: a review on microbial, enzymatic, nutritional and sensory quality and stability. Compr Rev Food Sci F 2013; 12: 455-467.

[4] Toepfl S. Pulsed electric field food processing - Industrial equipment design and commercial applications. Stewart Postharvest Review 2012; 8: 1-7.

[5] Charles-Rodriguez AV, Nevarez-Moorillon GV, Zhang QH, Ortega-Rivas E. Comparison of thermal processing and pulsed electric fields treatment in pasteurization of apple juice. Food Bioprod Process 2007; 85: 93-97.

[6] Álvarez JR, Sala FJ, Condón S. Inactivation of *Yersinia enterocolitica* by pulsed electric fields. Food Microbiol 2003; 20: 691-700.

[7] Bendicho S, Espachs A, Arantegui J, Martin O. Effect of high intensity pulsed electric fields and heat treatments on vitamins of milk. J Dairy Res 2002; 69: 113-123.

[8] Tseng SY, Wu TF, Wu MW. Bipolar narrow pulse generator with energy recovery feature for liquid food sterilization. IEEE T Ind Electron 2008; 55: 123-132.

[9] Toepfl S, Heinz V, Knorr D. Overview of pulsed electric field processing for food. In: Sun DW, editor. Emerging Technologies for Food Processing. London, UK: Elsevier Academic Press, 2005. pp. 69-99.

[10] Ghazala A, Schoenbach KH. Biofouling prevention with pulsed electric fields. IEEE T Plasma Sci 2000; 28: 115-121.

[11] Zou Y, Wang C, Peng R, Wang L, Hu X. Theoretical analyses of cellular transmembrane voltage in suspensions induced by high-frequency fields. Bio Elec Chem 2015; 102: 64-72.

[12] Wu TF, Tseng SY, Hung JC. Generation of pulsed electric fields for processing microbes. IEEE T Plasma Sci 2004; 32: 1552-1562.

[13] Premkumar E, Raji S. A simulation study of the electrical model of a biological cell. J Electrostat 2005; 63: 297-307.

[14] Pucihar G, Krmelj J, Rebersek M, Napotnik TB, Miklavcic D. Equivalent pulse parameters for electroporation. IEEE T Biomed Eng 2011; 58: 3279-3288.

[15] Goebel DM, Adler RJ, Beals DF, Reass WA. Pulser Technology. In: Anders A, editor. Handbook of Plasma Immersion Ion Implantation and Deposition. Hoboken, NJ, USA: Wiley, 2000. pp. 467-514.

[16] Glidden SC, Sanders HD. High voltage solid state trigger generators. In: IEEE 2005 Pulsed Power Conference; June 2005; Monterey, CA, USA. New York, NY, USA: IEEE. pp. 927-930.

[17] Schoenbach KH, Katsuki S, Robert HS, Buescher S, Stephen JB. Bioelectric—new applications for pulsed power technology. IEEE T Plasma Sci 2002; 30: 293-300.

[18] Merensky LM, Kardo-Sysoev AF, Flerov AN, Pokryvailo A, Shmilovitz D, Kesar AS. A low-jitter 1.8-kV 100-ps rise-time 50-kHz repetition-rate pulsed-power generator. IEEE T Plasma Sci 2009; 37: 1855-1862.

[19] Pokryvailo A, Yankelevich Y, Shapira M. A compact source of sub gigawatt sub-nanosecond pulses. IEEE T Plasma Sci 2004; 32: 1909-1918.

[20] Wu Y, Liu K, Qiu J, Liu X, Xiao H. Repetitive and high voltage Marx generator using solid-state devices. IEEE T Dielect El In 2007; 14: 937-940.

[21] Min RBD, Pavlov E, Kim JH. Repetitive nanosecond all solid state pulse generator using magnetic switch and SOS diodes. In: IEEE 2005 Pulsed Power Conference; June 2005; Monterey, CA, USA. New York, NY, USA: IEEE. pp. 1069-1072.

[22] Flisar K, Meglic SH, Morelj J, Golob J, Miklavcic D. Testing a prototype pulse generator for a continuous flow system and its use for *E. coli* inactivation and microalgae lipid extraction. Bio Elec Chem 2014; 100: 44-51.

[23] Kohler S, Levine ZA, Garcia-Fernandez MA. Electrical analysis of cell membrane poration by an intense nanosecond pulsed electric field using an atomistic-to-continuum method. IEEE T Microw Theory Tech 2015; 63: 2032-2040.

[24] Herman LN. A resonant pulse gate drive for high frequency applications. In: IEEE 1992 Applied Power Electronics Conference; February 1992; Boston, MA, USA. New York, NY, USA: IEEE. pp. 738-743.

[25] Yang RJ, Li SQ, Zhang QH. Effects of pulsed electric fields on the activity of enzymes in aqueous solution. Food Chem Toxicol 2004; 69: 241-248.

[26] Ren Y, Xu M, Lee FC. 12V VR efficiency improvement based on two-stage approach and a novel gate driver in the field of power electronics. In: IEEE 2005 Power Electronic Specialists Conference; June 2005; Recife, Brazil. New York, NY, USA: IEEE. pp. 2635-2641.

[27] Krishnaveni S, Rajini V. Resonant gate driver for series operation of MOSFETs. Energy Procedia 2017; 117C: 38-45.

[28] Grenier JR. Design of a MOSFET based pulsed power supply for electroporation. MSc, University of Waterloo, Waterloo, Canada, 2006.